Continuum-distorted-wave eikonal-initial-state description of the electron-impact ionization of H_2O at low impact energies

E. Acebal* and S. Otranto
Departamento de Física, Instituto de Física del Sur (IFISUR), Universidad Nacional del Sur (UNS), CONICET, Av. L. N. Alem 1253, B8000CPB - Bahía Blanca, Argentina

(Received 12 April 2018; published 5 July 2018)

Fully differential cross sections for electron impact of gaseous H_2O at an impact energy of 81 eV are calculated within the framework of the continuum-distorted-wave eikonal-initial-state model. Present results are benchmarked against recent experimental data obtained in MPIK-Heidelberg by means of a reaction microscope. Cross sections calculated for different molecular orientations are properly averaged to mimic the experimental conditions. Present results are in very good agreement with the experimental data for coplanar geometries. For the denominated perpendicular emission planes the agreement tends to deteriorate as the projectile momentum transfer increases.

DOI: 10.1103/PhysRevA.98.012703

I. INTRODUCTION

The understanding of the collision dynamics of electrons, ions, and photons with H_2O molecules is one of the major challenges faced by theoreticians and experimentalists working in the atomic and molecular collisions field. Given that these processes play a major role in many astrophysical contexts and can be used as a prototype for a biological medium, new insights on the acting physical mechanisms will benefit subsequent considerations regarding energy transport and radiation chemistry.

From the theoretical point of view, the workhorses for electron-impact ionization of complex molecules have been the distorted-wave methods such as the distorted-wave Born approximation (DWBA) (see [1] and references therein) and the Born-3C model [2,3]. This probably obeys the inherent complexity of these targets which makes difficult the implementation of numerically intensive methods that have been successful for light targets.

Although experimental research dates back to many decades ago, the first fully differential cross sections (FDCS) for electron-impact ionization of the valence orbitals of H_2O were reported by the Lohmann group [4]. In their study the impact energy was fixed at 250 eV and the analysis restricted to asymmetrical emission conditions in the collision plane (coplanar geometry). More recent studies considered symmetric and asymmetric emissions for the $1b_1$ orbital and symmetric coplanar and noncoplanar studies for the $3a_1$ orbital [5,6]. The development of the reaction microscope starting in the 1990s allowed the inspection of different collision processes at a kinematically complete level [7,8]. By 2003, a reaction microscope specially designed for electron-ionization studies was operational [9]. During the past few years, experimental techniques were developed that allow for simultaneously accessing a large fraction of the entire solid angle and a large range of energies of the continuum electrons in the final state [9,10], the entire angular acceptance for the slow ejected electron within the scattering plane [11], and, more recently, the measurements of internormalized cross sections [12]. These experimental improvements allow for a deeper evaluation of the strengths and weaknesses of the state-of-the-art theoretical models.

Last year, the Heidelberg group reported a kinematically complete study of electron-impact ionization of H_2O at the low projectile energy of 81 eV. In this study, electrons emitted from either the $1b_1$ or the $3a_1$ orbitals were measured in coincidence with the H_2O^+ ion [13]. Since the experimental setup does not discriminate the orbitals of origin of the detected electrons, the experimental cross sections are built upon the sum of the separate contributions from both orbitals. Results for three different emission planes were shown and compared to DWBA calculations by the Madison group to allow a full solid angle description. Based on the discrepancies observed, these authors concluded that second-order Born terms, not present in their treatment, might be relevant at this impact energy, particularly as one moves out from the coplanar geometry.

In this work, we analyze this recently reported set of data by means of the continuum-distorted-wave eikonal-initial-state (CDW-EIS) model in its three-body formulation. This model which now transits its fourth decade [14,15] has been systematically used with great success in the ion-atom [14–17] and ion-molecule [18,19] contexts and, in contrast to the DWBA or the simple Born initial state, it explicitly considers higher-order terms in the initial-state correlation. Interestingly, it has been scarcely applied in electron-ionization studies. In fact, Jones and Madison introduced it for the first time in two electron-hydrogen studies [20,21] by the end of the 1990s. Much more recently, it has been used to describe electron- and positron-impact ionization of Ar($3p$) [22–24]. At present we are not aware of any subsequent implementation of the model in electron-impact ionization studies.

In the next section we describe the main features of the theoretical model. In Sec. III we benchmark our methodology against the recently reported data. Conclusions are summarized in Sec. IV. Atomic units are used unless otherwise stated.

*emiliano.acebal@uns.edu.ar

II. THEORETICAL MODEL

The FDCS for the molecular orbital under consideration (either $1b_1$ or $3a_1$) in the CDW-EIS model and for a particular orientation of the molecular axes is given by

$$\frac{d^6\sigma}{dE\,d\Omega_1 d\Omega_2 d\alpha\,d\beta\,d\gamma} = N_e(2\pi)^4\frac{k_1k_2}{k_0}\left[\frac{1}{4}|T_{fi}^D + T_{fi}^E|^2 + \frac{3}{4}|T_{fi}^D - T_{fi}^E|^2\right]. \quad (1)$$

Here $N_e = 2$ represents the number of identical electrons in the molecular orbital, $\mathbf{k}_{1(2)}$ represents the momentum of the receding projectile and emitted electron, respectively, and $\mathbf{k}_0$ represents the impinging projectile momentum. T_{fi}^D indicates the direct amplitude and T_{fi}^E is the exchange amplitude $T_{fi}^E(\mathbf{k}_1,\mathbf{k}_2) = T_{fi}^D(\mathbf{k}_2,\mathbf{k}_1)$. The Gellman-Goldberger amplitude (T_{fi}) in Eq. (1) is represented in its *post* version by

$$T_{fi} = \langle\chi_f^-|W_f|\Psi_i^+\rangle + \langle\chi_f^-|V_i - W_f|\psi_i\rangle. \quad (2)$$

Here Ψ_i^+ is the exact scattering wave function developed from the unperturbed initial state ψ_i, with V_i being the initial-state perturbation. Different approximations to Ψ_i^+ lead to the DWBA, CDW-EIS, and distorted-wave models which consider a pure Born initial state. The wave function χ_f^- is an arbitrary distorted wave for the final state and W_f is the part of the Hamiltonian not solved by χ_f^-. In these functions the superscript (+) indicates outgoing-wave boundary conditions, while (−) refers to incoming-wave boundary conditions.

For the final-state wave function χ_f^- we employ the 3C wave function [25,26]

$$\chi_f^- = C^-(\mathbf{k}_1,\mathbf{r}_1)C^-(\mathbf{k}_2,\mathbf{r}_2)N^-(\alpha_3) \times {}_1F_1(i\alpha_3,1,-ik_{12}r_{12} - i\mathbf{k}_{12}\cdot\mathbf{r}_{12}). \quad (3)$$

The functions $C^-(\mathbf{k}_i,\mathbf{r}_i)$ are Coulomb waves defined by

$$C^-(\mathbf{k}_i,\mathbf{r}_i) = \frac{e^{i\mathbf{k}_i\cdot\mathbf{r}_i}}{(2\pi)^{3/2}}N^-(\alpha_i){}_1F_1(i\alpha_i,1,-ik_ir_i - i\mathbf{k}_i\cdot\mathbf{r}_i), \quad (4)$$

and α_i are the denominated Sommerfeld parameters $\alpha_i = \mu_{jk}Z_jZ_k/k_{jk}$, where $i \neq j \neq k = 1,2,3$. The overall normalization factor is given by

$$N = \prod_{i=1}^{3}N^-(\alpha_i) = \prod_{i=1}^{3}e^{-\frac{\pi}{2}\alpha_i}\,\Gamma(1 - i\alpha_i). \quad (5)$$

In our analysis we have used Coulomb waves corresponding to an H_2O^+ core charge equal to +1. A more appropriate final-state wave function, in physical terms, should take into account the multiple-center nature of the target.

The perturbation operators are $W_f = \nabla_1\cdot\nabla_{12} - \nabla_2\cdot\nabla_{12}$ and $V_i = -Z/r_1 + 1/r_{12}$. In order to be consistent with the core charge in the final state, we considered $Z = +1$.

In Eq. (2) there are two distinct initial wave functions that need to be taken into account. We denote with ψ_i the Born initial state

$$\psi_i = \frac{e^{i\mathbf{k}_0\cdot\mathbf{r}_1}}{(2\pi)^{3/2}}\varphi_i(\mathbf{r}_2) \quad (6)$$

and with Ψ_i^+ the eikonal initial state (EIS), which retains the effects of the long-range Coulomb potentials, and is given by

$$\Psi_i^+ = \frac{e^{i\mathbf{k}_0\cdot\mathbf{r}_1}}{(2\pi)^{3/2}}\varepsilon(\mathbf{r}_1)\varepsilon(\mathbf{r}_{12})\varphi_i(\mathbf{r}_2). \quad (7)$$

Here, $\varepsilon(\mathbf{r}_1)$ and $\varepsilon(\mathbf{r}_{12})$ are the eikonal phases

$$\varepsilon(\mathbf{r}_1) = e^{-\frac{iZ}{k_0}\ln(k_0r_1 - \mathbf{k}_0\cdot\mathbf{r}_1)},$$
$$\varepsilon(\mathbf{r}_{12}) = e^{\frac{i}{k_0}\ln(k_0r_{12} - \mathbf{k}_0\cdot\mathbf{r}_{12})}. \quad (8)$$

For the molecular orbital wave function $\varphi_i(\mathbf{r}_2)$ we make use of Moccia's self-consistent-field one-center-expanded molecular orbitals [27]. The basis set used in the expansion consists of Slater functions centered on the O atom.

As in our previous studies [22–24] in order to treat the continuum-continuum transition, we have used the wave-packet approach of Malcherek and Briggs [28]. The calculation of the transition amplitude at fixed molecular orientations has been developed by direct 6D numerical integration over

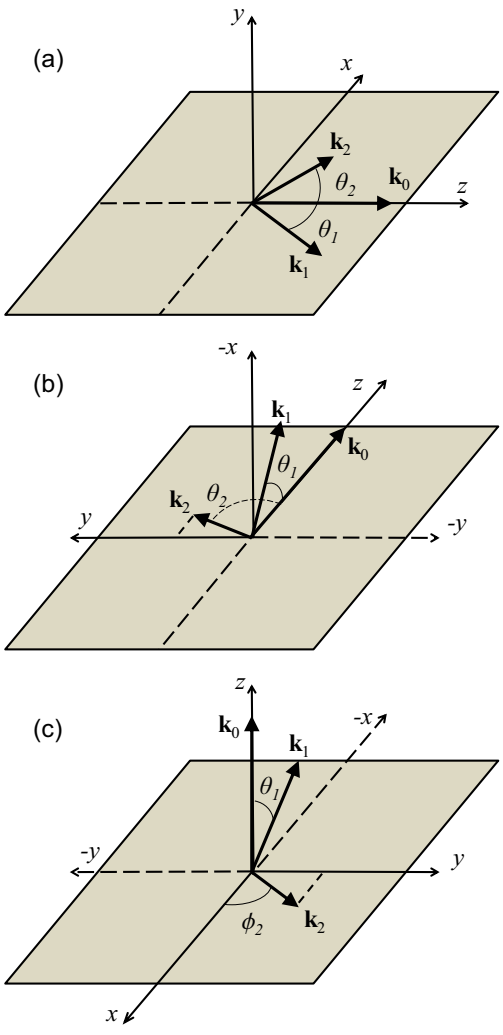

FIG. 1. Electron emission planes considered in this work: (a) collision plane xz, (b) semiperpendicular plane yz, and (c) full perpendicular plane xy. Both angles θ_1 and θ_2 were taken as positive counterclockwise.

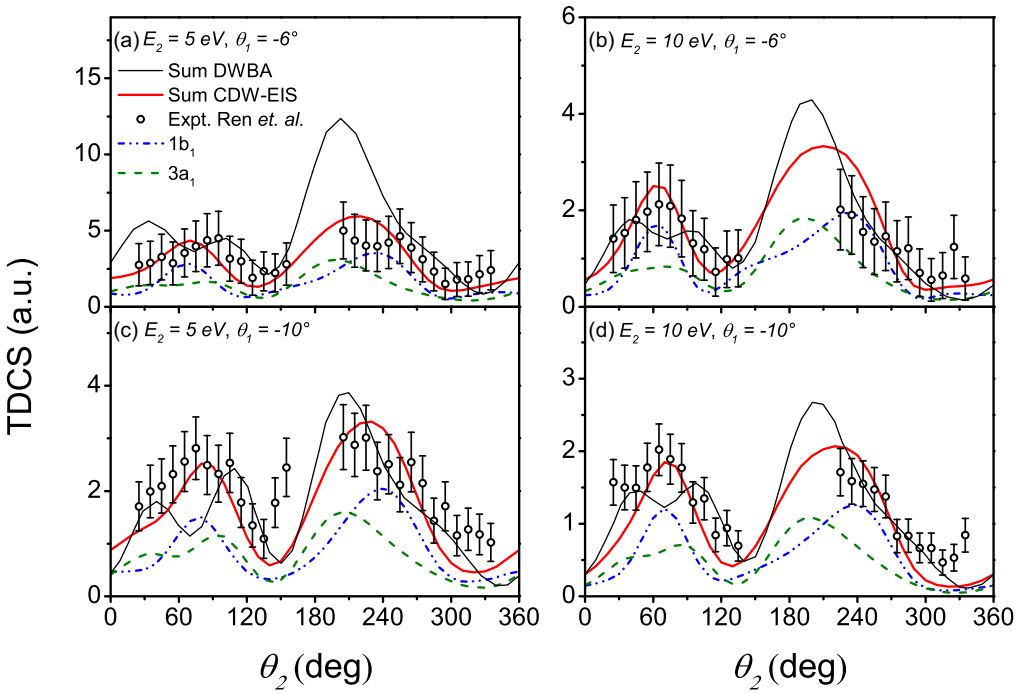

FIG. 2. CDW-EIS triply differential cross section for electron-impact ionization of $1b_1$ and $3a_1$ orbitals of H_2O. The impact energy is 81 eV. Emission energies and projectile scattering angles are indicated in the insets. Experimental and DWBA data from Ref. [13] scaled to the present theoretical results. Results shown are for the scattering plane xz [Fig. 1(a)].

the coordinates using an adaptive Monte Carlo scheme. We estimate our numerical uncertainty to be less than 5%.

The molecular orientation average procedure has been performed by numerically evaluating the integral

$$\frac{d^3\sigma}{dE\,d\Omega_1 d\Omega_2} = \frac{1}{8\pi^2}\int_0^{2\pi}\int_0^{\pi}\int_0^{2\pi} \frac{d^6\sigma}{dE\,d\Omega_1 d\Omega_2 d\alpha\,d\beta\,d\gamma} \times \sin\beta\,d\alpha\,d\beta\,d\gamma \tag{9}$$

over the three Euler angles α, β, and γ. Angular steps of 90° for α and γ and 30° for β were considered in our calculations after punctual checks of convergence using a denser mesh.

III. RESULTS

In this section we benchmark our data against the set of experimental data and the properly averaged DWBA calculations of Ref. [13]. Provided that the experimental data are relative and have been arbitrarily normalized to the DWBA theory, a common factor 0.8 is used to normalize the results of Ref. [13] to our theoretical results. In Fig. 1 we show the three emission planes considered: the collision or coplanar plane xz, the semiperpendicular plane yz, and the full perpendicular plane xy.

It is important to note that the DWBA approximation of Ref. [13] and the present CDW-EIS theory provide a similar physical picture for the outgoing stage of the collision process. That is a three-body continuum wave function, which is expressed as the product of three wave functions, each one for the different two-body subsystems. Both models explicitly consider the postcollisional interaction between the projectile electron and the emitted electron. It is on the entrance channel that these theories mainly differ. In the DWBA the projectile-target interaction is represented by means of a distorted wave which is a solution of a spherically symmetric potential corresponding to an asymptotically neutral target. Instead, in the CDW-EIS model the interaction between the projectile and the target components (active electron and target ion) in the initial state is described by means of a product of two eikonal phases, each of those corresponding to the asymptotic limit of a two-body Coulomb problem in the continuum. In other words, the projectile distinguishes, even asymptotically, the Coulomb fields of the active electron and the target ion while it approaches the target. In this sense, CDW-EIS contains higher-order terms in the initial-state correlation compared to DWBA. These terms are expected to play an increasing role as the projectile impact energy decreases.

First, in Fig. 2 we focus on the triply differential cross sections (TDCS) corresponding to the collision plane. It can be seen that in all cases the CDW-EIS model provides a very good description of the experiment. The DWBA predicts a two-peak binary structure mainly arising from the $1b_1$ contribution. In contrast, CDW-EIS predicts a single peak binary structure and a recoil to the binary peak ratio that is in better agreement with the experiment. The same situation stands for the four geometries reported. Our $1b_1$ contribution leads to a single peak binary structure at the projectile momentum-transfer value explored. We note that previous theoretical studies on electron- and positron-impact ionization of Ar($3p$) indicated that a transition from single to double binary peaks takes place when the projectile momentum transfer increases [23]. Provided that the $1b_1$ and $3a_1$ orbitals are mostly $2p$ in nature, future theoretical and experimental research should be directed to learn whether these assertions which were formulated for Ar targets also apply for the H_2O case or not.

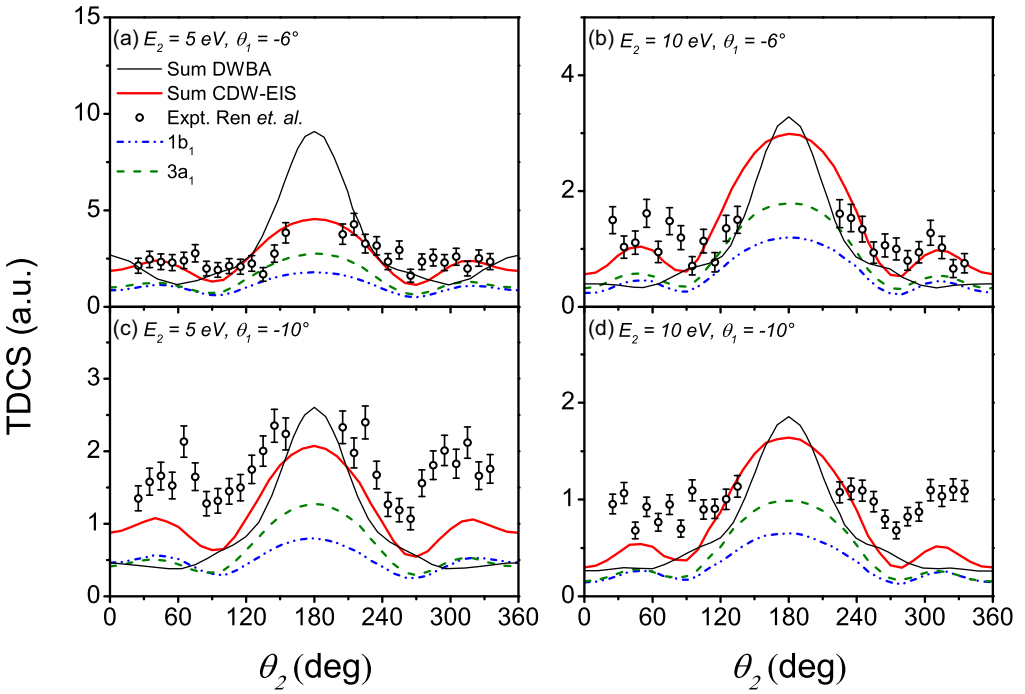

FIG. 3. Same as Fig. 2, but for the semiperpendicular plane *yz* [Fig. 1(b)].

The semiperpendicular plane [Fig. 1(b)] case is considered in Fig. 3. Symmetry considerations require structures to be symmetric around $\theta_2 = 180°$. This plane intersects the collision plane at $\theta_2 = 0°$ ($\theta_2 = 180°$), which corresponds to the same angular values for θ_2 in the collision plane. In this sense, the structure at $\theta_2 = 0°$ in the semiperpendicular plane can be related to the left tail of the binary peak and the structure at $\theta_2 = 180°$ can be related to the left part of the recoil peak in the collision plane. At the smaller momentum transfers, i.e., at small scattering angles [Fig. 3(a) and Fig. 3(b)], CDW-EIS results are in good agreement with the data. Further quantitative analysis of its behavior right on the central peak is not feasible due to the lack of experimental data in the beam direction. As the momentum transfer increases [Fig. 3(c) and Fig. 3(d)], CDW-EIS underestimates the experimental data but retains the correct description of the structures, in particular the angular positions of the minima and maxima.

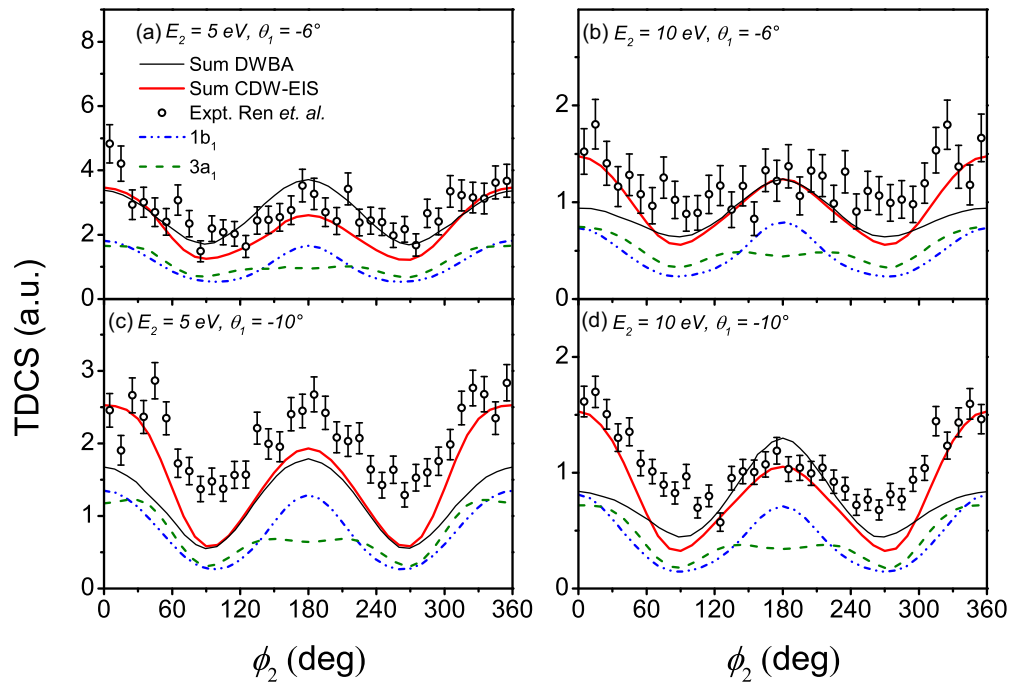

FIG. 4. Same as Fig. 2. but for the full perpendicular plane *xy* [Fig. 1(c)].

Finally, in Fig. 4 we report our CDW-EIS results for the full perpendicular plane [Fig. 1(c)]. Symmetry considerations again require structures to be symmetric around $\phi_2 = 180°$. This plane intersects the collision plane at $\phi_2 = 0°$ ($\phi_2 = 180°$) which corresponds to $\theta_2 = 90°$ ($\theta_2 = 270°$) in the collision plane. Hence the structure at $\phi_2 = 0°$ in the full perpendicular plane can be related to the maximum of the binary peak and the structure at $\phi_2 = 180°$ can be related to the right part of the recoil peak in the collision plane. Again, we find good overall agreement between the CDW-EIS theory and the experimental data. In Figs. 4(c) and 4(d) the data at the minima are underestimated, suggesting as in the previous case that the exploration of collision geometries involving increasing momentum transfers would provide a route to further test the theoretical models under use.

IV. CONCLUSIONS

In this work we have reported CDW-EIS calculations of TDCS for electron-impact ionization of H_2O at the low impact energy of 81 eV. These have been benchmarked against recently reported experimental data measured in a reaction microscope and theoretical data obtained in the framework of the DWBA model.

Present results are in good agreement with the experimental data and suggest at first sight that the inclusion of the initial-state distortion, at least asymptotically, provides a much better description of the collision process at low impact energies compared to formulations which consider the projectile-target interaction at first order. However, more detailed analyses are needed to confirm or establish boundaries for this preliminary assessment. It is our hope that the results shown here will stimulate further experimental and theoretical work in the area.

ACKNOWLEDGMENTS

This work has been supported by Grant No. PGI 24/F073, Secretaría General de Ciencia y Tecnología, Universidad Nacional del Sur (Argentina). We thank Dr. Alexander Dorn and Dr. Xueguang Ren for providing us with the experimental data in tabular form and Dr. S. Martinez and Lic. N. Bachi for a critical reading of the manuscript.

[1] D. H. Madison and O. Al-Hagan, J. At. Mol. Opt. Phys. **2010**, 367180 (2010).
[2] C. Champion, C. Dal Cappello, S. Houamer, and A. Mansouri, Phys. Rev. A **73**, 012717 (2006).
[3] M. L. de Sanctis, M.-F. Politis, R. Vuilleumier, C. R. Stia, and O. A. Fojón, J. At. Mol. Opt. Phys. **48**, 155201 (2015).
[4] D. S. Milne-Brownlie, S. J. Cavanagh, B. Lohmann, C. Champion, P. A. Hervieux, and J. Hanssen, Phys. Rev. A **69**, 032701 (2004).
[5] C. Kaiser, D. Spieker, J. Gao, M. Hussey, A. Murray, and D. H. Madison, J. Phys. B: At., Mol., Opt. Phys. **40**, 2563 (2007).
[6] K. L. Nixon, A. J. Murray, O. Al-Hagan, D. H. Madison, and C. Ning, J. Phys. B: At., Mol., Opt. Phys. **43**, 035201 (2010).
[7] V. Mergel, R. Dörner, J. Ullrich, O. Jagutzki, S. Lencinas, S. Nüttgens, L. Spielberger, M. Unverzagt, C. L. Cocke, R. E. Olson, M. Schulz, U. Buck, E. Zanger, W. Theisinger, M. Isser, S. Geis, and H. Schmidt-Böcking, Phys. Rev. Lett. **74**, 2200 (1995).
[8] R. Dörner, H. Bräuning, J. M. Feagin, V. Mergel, O. Jagutzki, L. Spielberger, T. Vogt, H. Khemliche, M. H. Prior, J. Ullrich, C. L. Cocke, and H. Schmidt-Böcking, Phys. Rev. A **57**, 1074 (1998).
[9] J. Ullrich, R. Moshammer, A. Dorn, R. Dörner, L. Schmidt, and H. Schmidt-Böcking, Rep. Prog. Phys. **66**, 1463 (2003).
[10] M. Dürr, C. Dimopoulou, A. Dorn, B. Najjari, I. Bray, D. V. Fursa, Z. Chen, D. H. Madison, K. Bartschat, and J. Ullrich, J. Phys. B: At., Mol., Opt. Phys. **39**, 4097 (2006).
[11] M. A. Stevenson and B. Lohmann, Phys. Rev. A **77**, 032708 (2008).
[12] T. Pflüger, O. Zatsarinny, K. Bartschat, A. Senftleben, X. Ren, J. Ullrich, and A. Dorn, Phys. Rev. Lett. **110**, 153202 (2013).
[13] X. Ren, S. Amami, K. Hossen, E. Ali, C. G. Ning, J. Colgan, D. Madison, and A. Dorn, Phys. Rev. A **95**, 022701 (2017).
[14] D. S. F. Crothers and J. S. McCaan, J. Phys. B: At. Mol. Phys. **16**, 3229 (1983).
[15] P. D. Fainstein, V. H. Ponce, and R. D. Rivarola, J. Phys. B: At., Mol., Opt. Phys. **34**, 3091 (1991).
[16] L. Gulyás, P. D. Fainstein, and A. Salin, J. Phys. B: At., Mol., Opt. Phys. **28**, 245 (1995).
[17] M. D. Sánchez, W. R. Cravero, and C. R. Garibotti, Phys. Rev. A **61**, 062709 (2000).
[18] S. Bhattacharjee, S. Biswas, J. M. Monti, R. D. Rivarola, and L. C. Tribedi, Phys. Rev. A **96**, 052707 (2017).
[19] S. Bhattacharjee, C. Bagdia, M. R. Chowdhury, J. M. Monti, R. D. Rivarola, and L. C. Tribedi, Eur. Phys. J. D **72**, 15 (2018).
[20] S. Jones and D. H. Madison, Phys. Rev. Lett. **81**, 2886 (1998).
[21] S. Jones and D. H. Madison, Phys. Rev. A **62**, 042701 (2000).
[22] S. Otranto, Phys. Rev. A **79**, 012705 (2009).
[23] S. Otranto and R. E. Olson, Phys. Rev. A **80**, 012714 (2009).
[24] O. G. de Lucio, S. Otranto, R. E. Olson, and R. D. DuBois, Phys. Rev. Lett. **104**, 163201 (2010).
[25] C. R. Garibotti and J. E. Miraglia, Phys. Rev. A **21**, 572 (1980).
[26] M. Brauner, J. S. Briggs, and H. Klar, J. Phys. B: At., Mol., Opt. Phys. **22**, 2265 (1989).
[27] R. Moccia, J. Chem. Phys. **40**, 2186 (1964).
[28] A. W. Malcherek and J. S. Briggs, J. Phys. B: At., Mol., Opt. Phys. **30**, 4419 (1997).